Single-shot 3-D wide-field fluorescence imaging with a computational miniature mesoscope

November 2 2020, by Thamarasee Jeewandara

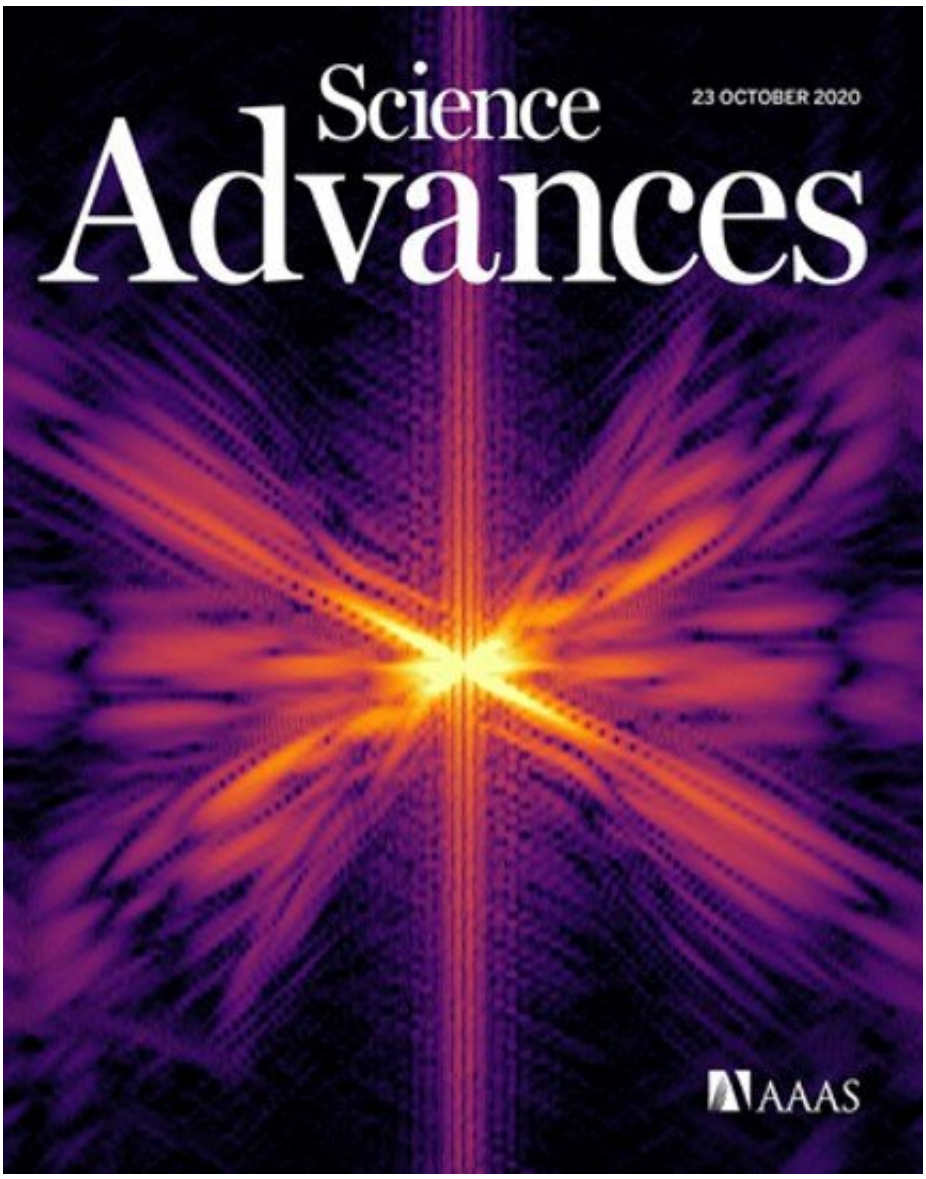

Online cover - a Computational Miniature Mesoscope (CM2). Image credit: Xue et al., Science Advances, doi:10.1126/sciadv.abb7508

The online feature cover photograph on *Science Advances* this week displays fluorescence imaging with a computational miniature mesoscope (CM^2). The technique of fluorescence imaging is an essential tool for biologists and neuroscientists; however, conventional microscopes and miniaturized microscopes (miniscopes) are constrained by limited space-bandwidth product—a measurement of the information capacity of an optical system, shallow depth of field and an inability to resolve three-dimensional (3-D) distributed emitters. To overcome existing limits, Yujia Xue and a team of researchers in electrical and computer engineering, biology, neurophotonics and biomedical engineering at Boston University, U.S., developed a light and compact mesoscope known as the computational miniature mesoscope (CM^2).

The new platform integrated a microlens for imaging and an LED array for excitation within the same setup. The device performed single-shot 3-D imaging and facilitated a 10-fold field-of-view gain and a 100-fold depth-of-field improvement, compared to existing miniscopes. Xue et al. tested the device with fluorescent beads and fibers alongside phantom experiments to measure the effects of bulk scattering and background fluorescence. The team discusses the practicality of this mesoscope for broad applications in biomedicine and 3-D neural recording.

Advancing fluorescence microscopy

Fluorescence microscopy is a key technique in fundamental biology and systems neuroscience. Recent technological developments are aimed at overcoming barriers of scale to investigate individual neurons of only a few microns in size. For example, macroscopes, mesolens microscopes

and two-photon microscopes have begun to bridge this scale; however, the development of such imaging systems is limited by scale-dependent geometric aberrations of optical elements. The achievable field of view (FOV) is also limited by the system's shallow depth of field in many bioimaging applications. Researchers are also focused on miniaturizing the technology to allow in vivo imaging in freely behaving animals. For example, miniaturized microscopes known as 'miniscopes' have gained unprecedented access to neural signals, although the systems remain restricted by their optics, much like their fluorescence microscopy counterparts. Xue et al. therefore introduced and demonstrated a computational miniature microscope (CM^2) with large-scale, 3-D fluorescence measurements on a compact, light-weight platform.

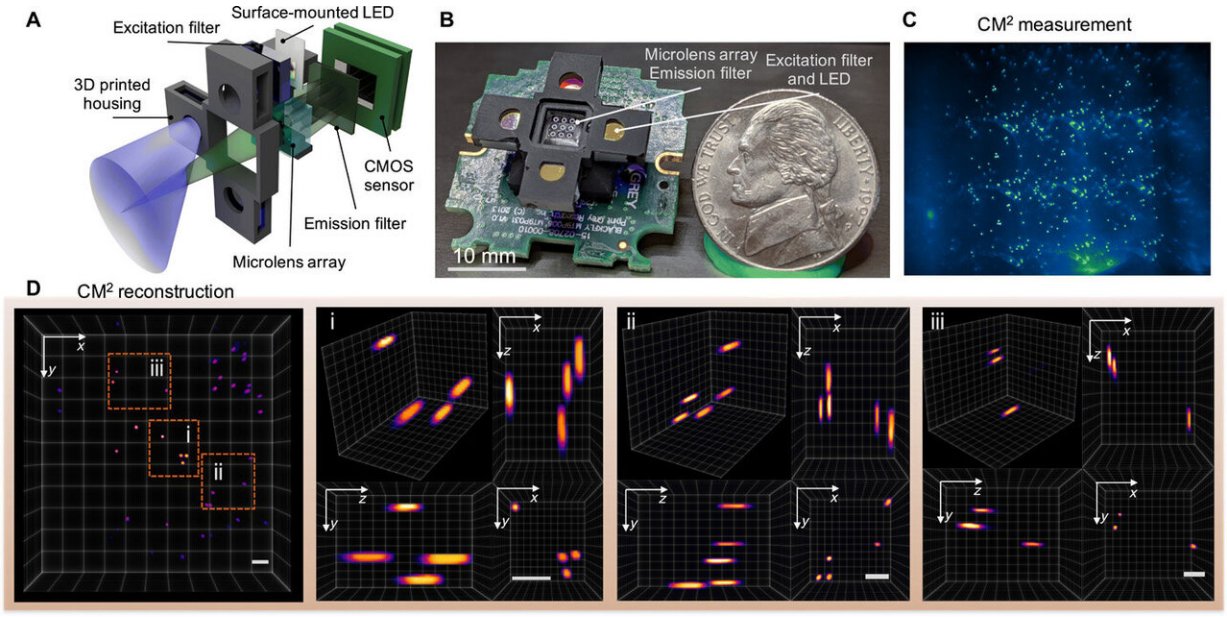

Single-shot 3D fluorescence CM2. (A) The CM2 combines an MLA optics and light-emitting diode (LED) array excitation in a compact and lightweight platform. (B) Picture of the CM2 prototype (the electric wires and the sensor driver are omitted). Photo credit: Yujia Xue, Boston University. (C) CM2 measurement on 100-μm fluorescent particles suspended in clear resin. (D) Projected view of the CM2 reconstructed volume (7.0 mm by 7.3 mm by 2.5

mm) and three zoom-in regions with orthogonal views. Scale bars, 500 μm. CMOS, complementary metal-oxide semiconductor. Credit: Science Advances, doi: 10.1126/sciadv.abb7508

The mechanism-of-action of the computational miniature mesoscope (CM^2)

The team used simple optics in the setup to accomplish space-bandwidth product (SBP) improvement and 3-D imaging capabilities without the need for mechanical scanning. The technique bypassed the physical limits of the integrated optics by jointly designing the hardware and the algorithm. The CM^2 imaging method combined several different features of microscopic imaging, such as integral imaging, light-field microscopy and coded aperture imaging. In its mechanism of action, the microscope collected a single 2-D measurement using a microlens array (MLA) for subsequent computational reconstruction of the 3-D fluorescence distribution.

The CM^2 used the microlens array as the sole imaging element and allowed the setup to overcome the field-of-view (FOV) limits imposed by the objective lens of conventional microscopes. The CM^2 algorithm solved the 2-D-to-3-D deconvolution problem to provide depth-resolved reconstructions. Xue et al. explained the principle of the CM^2 single-shot 3-D imaging capability by drawing an analogy to frequency division multiplexing (FDM). The team then quantified the achievable resolution of the CM^2 by computing the 3-D modulation transfer function (MTF) of the system and analyzing the lateral resolution.

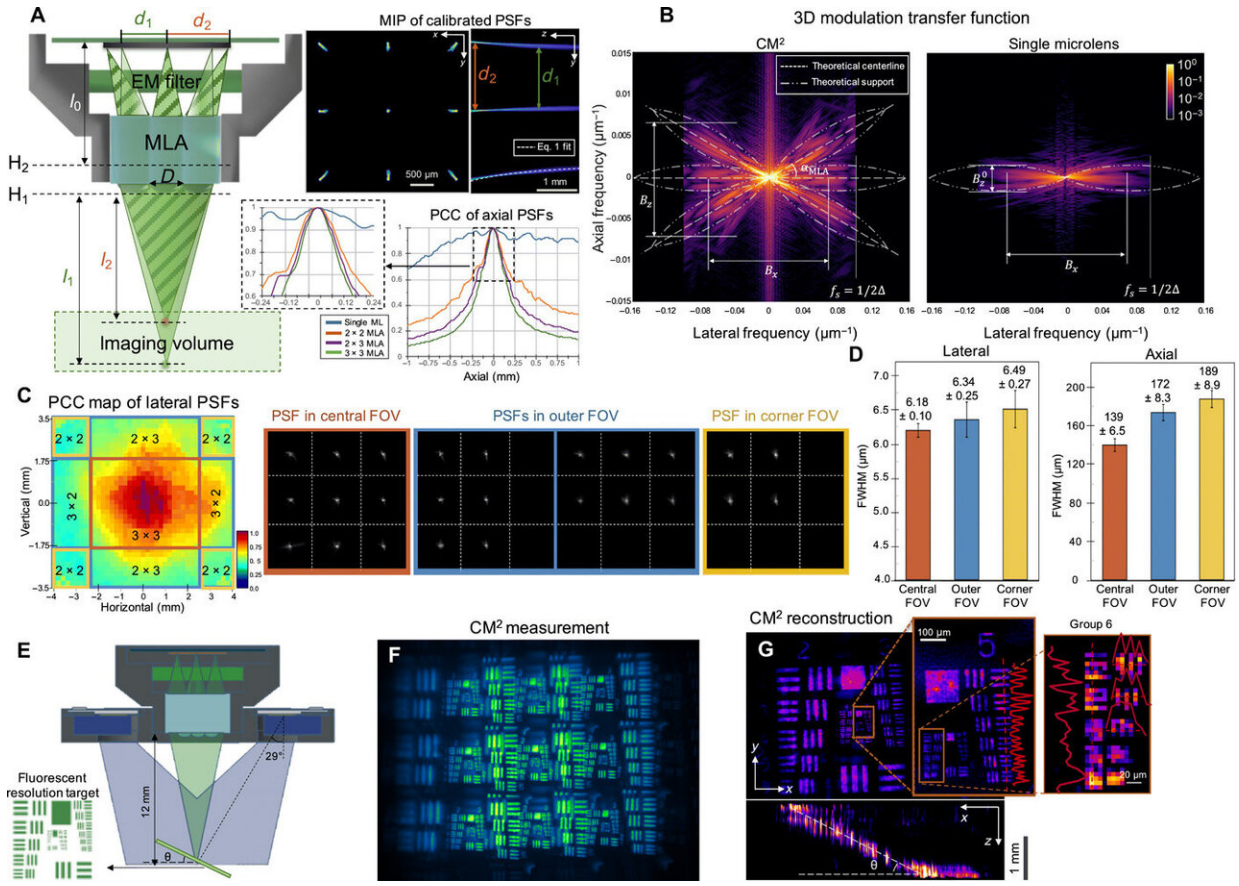

Characterization of the CM2's imaging principle, shift variance, and resolution. (A) The CM2 produces axially varying array PSFs to achieve optical sectioning. The axial shearing in the side foci is well characterized by the geometric model presented in the study. The PCC of the axially scanned PSFs quantifies the expected axial resolution. EM, emission. (B) The 3D MTF (shown in log scale) shows that the CM2 captures extended axial frequency information and enlarges the system's SBP. The support of the experimental MTF matches with the theory (in dashed-dotted curve). The angle of each tilted "band" in the MTF is set by the angular location of the corresponding microlens αMLA (in dashed line). (C) The lateral shift variance is characterized by the PCC of the laterally scanned PSFs. The PSF in the central FOV (marked by orange boundary lines) contains 3 × 3 foci; the PSF in the outer FOV (marked by blue boundary lines) contains 2 × 3 or 3 × 2 foci; the PSF in the corner FOV (marked by yellow boundary lines) contains 2 × 2 foci. (D) The resolution at different regions of the FOV is characterized by reconstructing a 5-μm pinhole object using the CM2's shift-invariant model. The lateral full width at half maximum (FWHM) is consistently

below 7 μm. The axial FWHM is ~139 μm in the central FOV and degrades to ~172 and ~ 189 μm in the outer and corner FOVs, respectively. (E) Geometry for imaging a tilted fluorescent target. (F) Raw CM2 measurement. (G) MIPs of the reconstructed volume (8.1 mm by 5.5 mm by 1.8 mm). The 7-μm features (group 6, element 2) can be resolved as shown in the zoom-in xy projection. The axial sectioning capability is characterized by the xz projection, validating the feature size–dependent axial resolution. Credit: Science Advances, doi: 10.1126/sciadv.abb7508

Proof-of-concept experiments

Xue et al. approximated the image formation of the CM^2 setup by using a slice-wise shift-invariant model. They characterized the resolution and lateral shift variance of the setup prior to experimental imaging and imaged a fluorescent resolution target to validate the lateral resolution of the CM^2. They validated the observations using Zemax-simulated measurements to find a good agreement between the simulations and the experiments. The new platform allowed the scientists to localize fluorescent emitters distributed across a large volume. They tested the performance of CM^2 on samples with a feature size similar to a single neuron. During these experiments, the CM^2 algorithm was tolerant of signal degradations such as reduced signal-to-noise ratios to enable high-quality, full-field-of-view reconstruction. The team compared the CM^2 reconstruction and an axial stack acquired by an objective lens to demonstrate the accuracy of single-shot localization of individual particles.

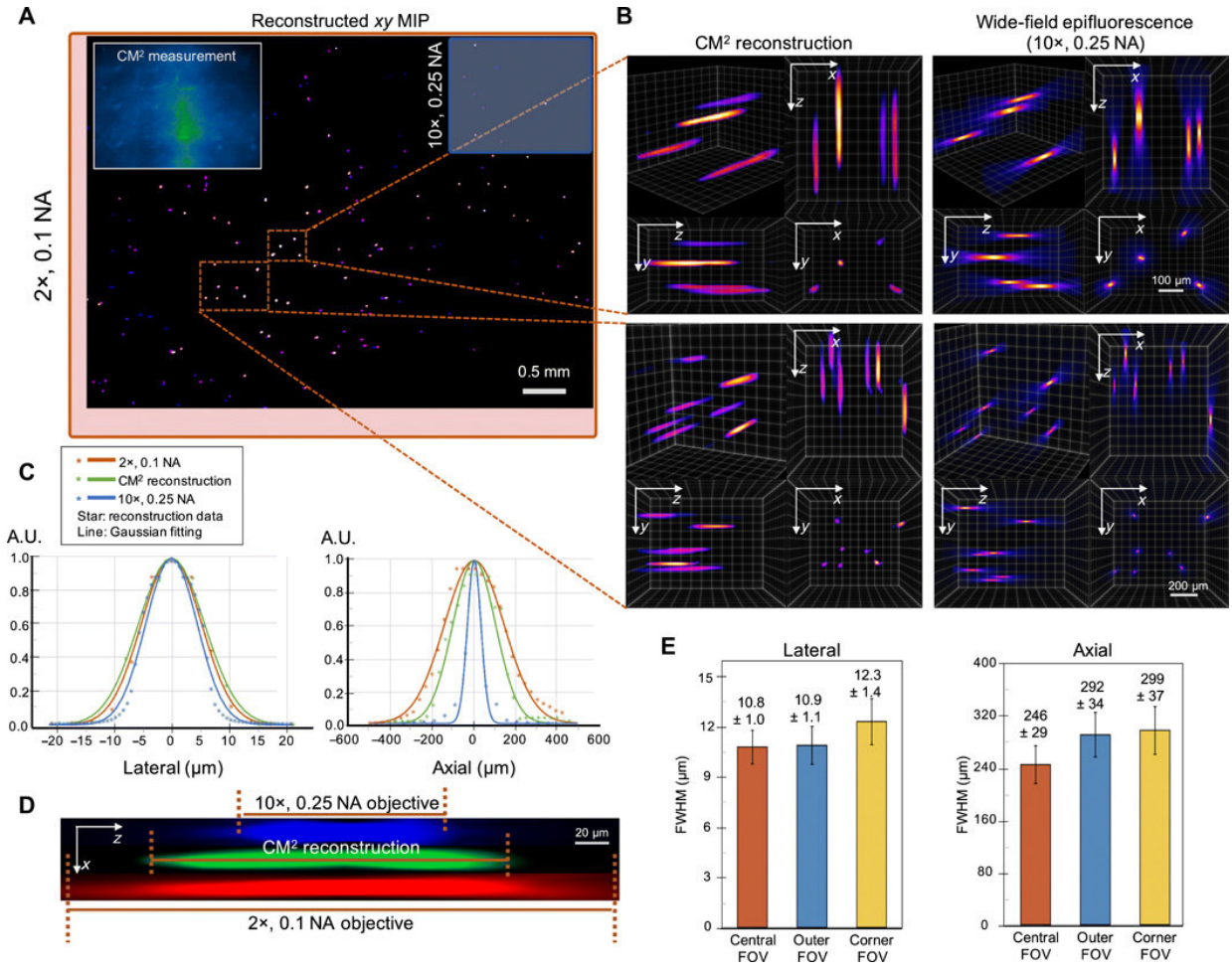

Single-shot 3D imaging of 10-μm fluorescent particles in a clear volume. (A) xy MIP of the reconstructed volume spanning 5.7 mm by 6.0 mm by 1.0 mm. Top left inset: Raw CM2 measurement. The FOV of the CM2is comparable to a 2× objective lens (red bounding box) and is ~25× wider than the 10× objective lens (blue bounding box). (B) Zoom-in of the CM2 3D reconstruction benchmarked by the axial stack taken by a 10×, 0.25 NA objective lens. (C) Lateral and axial cross sections of the recovered 10-μm particle. By comparing with the measurements from the standard wide-field fluorescence microscopy, the CM2 faithfully recovers the lateral profile of the particle and achieves single-shot depth sectioning. A.U., arbitrary units. (D) xz cross-sectional view of a reconstructed fluorescent particle, as compared to the axial stack acquired from the 2× and 10× objective lenses. (E) To characterize the spatial variations of the reconstruction, the statistics of the lateral and axial FWHMs of the reconstructed particles are plotted for the central, outer, and corner FOV. The lateral width

changes only slightly (~0.9%) in the outer FOV but increases in the corner FOV (~13.9%). The axial elongation degrades from ~246 μm in the central FOV to ~292 and ~ 299 μm in the outer and corner FOV regions, respectively. Credit: Science Advances, doi: 10.1126/sciadv.abb7508

Experiments on fluorescent fibers on a curved surface and on controlled scattering phantoms.

The scientists next tested the ability to image complex volumetric fluorescent samples on fluorescent fibers spread on a 3-D printed curved surface, mimicking the surface profile of a mouse cortex, spanning a wide field-of-view and an extended depth. The algorithm accurately recovered the in-focus structures and solved for the 3-D object, while resolving most of the individual fibers. The team further conducted experiments on eight imaging phantoms to test the performance of CM^2 under bulk scattering and strong background fluorescence. During the experiments, they seeded all phantoms with the same concentration of target fluorescent particles and credited the differences in reconstruction to bulk scattering and background fluorescence. The team then included 1.1-μm background fluorescent particles to mimic unresolvable fluorescent sources commonly seen on biological samples; such as neutropils in the brain. They quantified the scattering level for each phantom, performed 3-D reconstruction for each scattering phantom and performed all deconvolutions using the same computational setting. The estimated reconstruction depth range varied with surface variations present in each phantom.

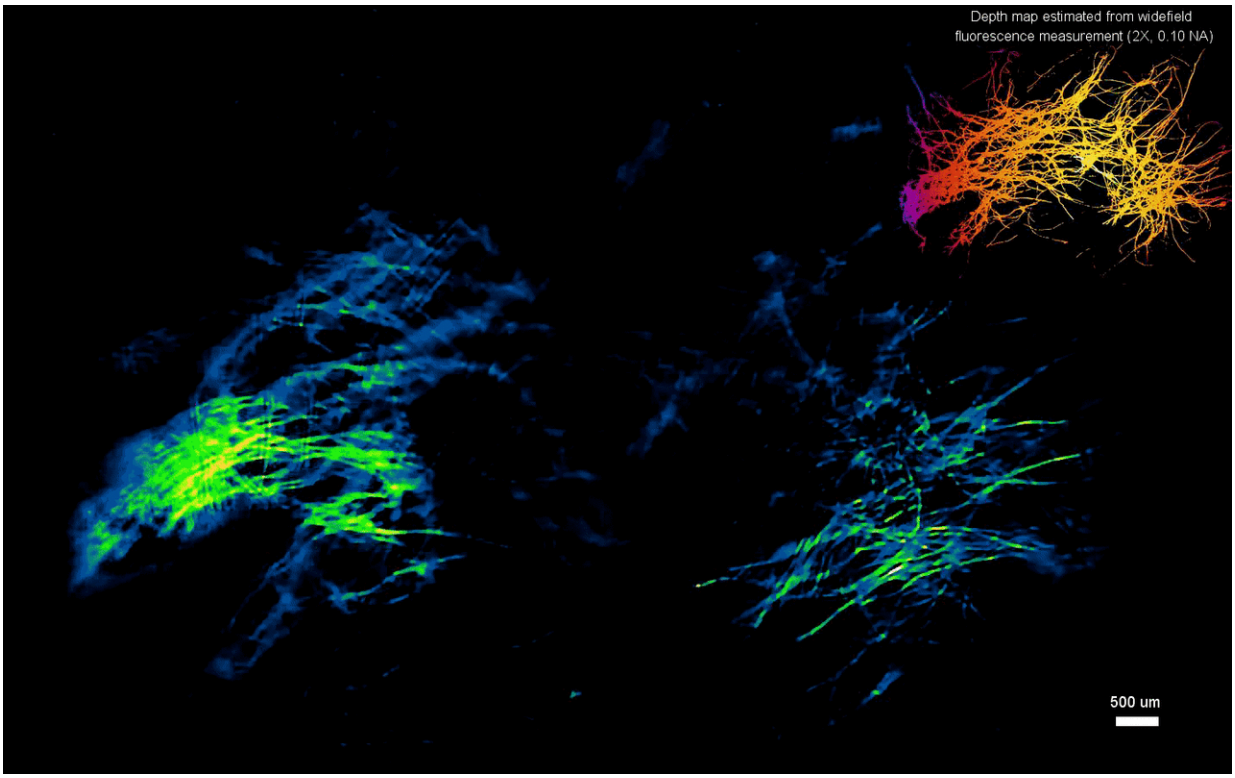

Reconstruction of fluorescent fibers. The movie file visualizes the volumetric reconstruction of fluorescent fibers on a curved surface. For comparison, the depth map estimated from the focal stack from a widefield epi-fluorescence microscope with a 2×, 0.1 NA objective lens is displayed. Credit: Science Advances, doi: 10.1126/sciadv.abb7508

In this way, Yujia Xue and colleagues developed a new miniaturized fluorescence imaging system to allow single-shot mesoscopic 3-D imaging. The computational miniature mesoscope (CM^2) method integrated fluorescence imaging and the excitation modules on the same compact platform. The team presented the simulations and experiments to establish the mechanism of action and 3-D imaging capacity of the CM^2. They simulated brain-wide imaging of vascular networks and the primary results were promising. The CM^2 prototype is not yet comparable to head-mounted in vivo applications (on animal models) in

neuroscience labs, although the team envision optimizing the device for full-cortical in vivo imaging in freely moving mice. The imaging device can be further improved with further developments in hardware and algorithms to open new and exciting opportunities within in vivo neural recording and biomedical applications.

More information: Yujia Xue et al. Single-shot 3D wide-field fluorescence imaging with a Computational Miniature Mesoscope, *Science Advances* (2020). DOI: 10.1126/sciadv.abb7508

Jeff W Lichtman et al. Fluorescence microscopy, *Nature Methods* (2005). DOI: 10.1038/nmeth817.

Sofroniew N. J. et al., A large field of view two-photon mesoscope with subcellular resolution for in vivo imaging, *eLife*, doi.org/10.7554/eLife.14472.001